Sustainable Energy Technologies and Assessments 53 (2022) 102696

Contents lists available at ScienceDirect

Sustainable Energy Technologies and Assessments

journal homepage: www.elsevier.com/locate/seta

IoT battery management system in electric vehicle based on LR parameter estimation and ORMeshNet gateway topology

P. Santhosh Kumar [a], Rajesh N. Kamath [b], Prasanthi Boyapati [c], P. Joel Josephson [d], L. Natrayan [e], Finney Daniel Shadrach [f,*]

[a] Department of IT, SRM Institute of Science and Technology, Ramapuram, India
[b] Mangalore Institute of Technology & Engineering, Moodabidri, India
[c] Department of Computer Science and Engineering, R.V.R&J.C College Of Engineering, Guntur, Andhra Pradesh, India
[d] Department of Electronics and Communication Engineering, St Martin's Engineering College, Secunderabad, Telangana, India
[e] Department of Mechanical Engineering, Saveetha School of Engineering, SIMATS, Chennai, Tamil Nadu, India
[f] Department of ECE, KPR Institute of Engineering and Technology, Coimbatore, India

ARTICLE INFO

Keywords:
Electric vehicle (EV)
Battery management system (BMS)
State of change (SOC)
State of Health (SOH)
State of power (SOP)
Lasso regularization (LR)
Equivalent circuit model (ECM)
Optimal tuned Hyperparameter based artificial jellyfish search (OTH-AJS)
Logit Normal distribution based Bald eagle search (LND-BES)
Optimal routing Mesh networking (ORMeshNet)

ABSTRACT

Over the last few years, electric cars (EVs) have grown in popularity. The battery management system (BMS) is critical to the long-term viability and smooth operation of an electric vehicle. The management of electric vehicles' batteries daily may help them operate better. All battery-related data is monitored and transmitted to the cloud in real time for monitoring via the Internet of Things, which is completely automated. Open loop approaches for predicting SOC, SOH, and SOP parameters suffer from a decrease in reliability when current sensor uncertainties and the rarity of relaxation status are addressed. Also, keep in mind that IoT network nodes are generally delay-tolerant, and message delivery latency still has a substantial impact on monitoring an electric vehicle's battery system. (EV). The research team created an Internet of Things BMS based on LR parameter estimation and an ORMeshNet gateway topology to address this issue. Before any other systems can be monitored or diagnosed with the BMS or any other system, techniques are first created based on an LR to estimate SOC and SOH accurately and efficiently. This method achieves a higher rate of convergence as well as a higher level of fault tolerance than other estimation methods. The updated parameters and estimated states are used for the SOP estimator to provide more accurate peak power estimates while fulfilling operational constraints of the battery current, voltage, and SOC. Thereafter, the estimated results are transferred via IoT platform that comprises of OTH-AJS node selection followed with LND-BES optimal routing based MeshNet gateway protocol to transfer the data for monitoring. The proposed approach yields a throughput of 88.97%, a PDR of 87.98%, and a Goodput of 83.98%. Experimental results show enormous improvement in estimating the parameters with better throughput, PDR, and goodput value as compared to existing methods.

Introduction

Electric Vehicles (EVs) are already accustomed to a wide variety of battery chemistries with different specifications, and this trend is anticipated to continue. BMS (Battery Management System) is offered to monitor the operational system, performance, as well as battery life, including the charge and discharge process [1,2]. It includes a variety of tools for measuring battery voltage, current, and temperature, among other things. These statistics can be used to identify the battery's state of charge (SOC) and health (SOH). The battery management system (BMS) is a critical component of an electric vehicle since it guarantees that the battery functions efficiently and lasts a long time [3]. Electric vehicles (EVs) use lithium-ion cells in their battery packs, which are constructed into modules and connected in series to create the voltage needed for the vehicle's operation. Lithium-ion batteries as electrical devices must work securely within a small voltage and temperature range due to their great sensitivity [4,5].The cell may degenerate if its temperature or voltage fall below the required range. The inside temperature of the battery can vary by more than 12 degrees Celsius, making it more difficult to measure than the surface temperature. However, by keeping an eye on the internal temperature, BMS can reduce energy use, prevent fires and explosions, and better understand the consequences of ageing.

* Corresponding author.
E-mail addresses: bprasanthi@rvrjc.ac.in (P. Boyapati), pjoelece@smec.ac.in (P. Joel Josephson).

https://doi.org/10.1016/j.seta.2022.102696
Received 24 March 2022; Received in revised form 13 August 2022; Accepted 14 August 2022

Micro temperature sensor internal temperature measurement is often difficult and expensive. Another crucial task that a BMS must reliably do is measuring voltage. Each BMS cell must have at least one voltage acquisition channel to determine the current voltage level. These chips have a resolution of 380 V and an accuracy of 1 mV, which ranges from 12 to 16 bits. Voltage measurements are also critical in determining SOC. If these values exceed the set maximum, the cell may be destroyed. For a common Lithium-Ion cell, the voltage and temperature must not exceed [2.5; 4.2] V and [13; 60] C, respectively [6,7]. The safety window refers to the range of values within which a cell is safeguarded from damage. Multidisciplinary research is needed to address severe concerns regarding the safety, dependability, and degradation of Li-ion batteries, but also to examine strategies to minimise system costs while ensuring battery energy storage systems run as effectively as feasible [8,9]. These initiatives include the creation of fresh batteries and cutting-edge battery management systems (BMS). Extreme/normal cell voltage restrictions the entire battery pack must have a structure to oversee, control, maintain, and manage these requirements. The battery management system (BMS) is the battery pack's "brain" (BMS). A good battery management system will keep the battery safe, anticipate its lifespan, regulate charging and discharging, and figure out how many cycles it will go through before it needs to be recharged again. Thermal conditions must be controlled, module or pack currents must be organised, SOC and SOH must be measured, and cells must be altered to slow down cell degradation. To ensure safe battery operation, optimise battery control, offer maximum force, and extend battery life, a robust BMS is required. A BMS must connect with other onboard components, such as the engine control module, temperature control module, common bus bar, monitoring system, and car computer, to perform a wide range of functions on the vehicle.

Due to recent advances in IoT and cloud computing resources, it is expected that the design and operation of large-scale battery energy storage systems will undergo a paradigm shift [10] due to the continuous research into these technologies [11,12]. New cloud-connected battery management systems for tiny electric vehicles and cloud battery analytics services have been created in recent years [13,14] to speed up the development of battery products. However, the implementation of a building management system (BMS) on an IoT platform is extremely complicated. In contrast, considering the cumulative error supplied by current sensor uncertainties as well as the rarity of relaxation status has been shown to decrease the dependability of these open-loop algorithms for predicting the SOC, SOH, and SOP parameters [15,16]. [15,16] As a result, IoT nodes are frequently delay-tolerant, and message delivery latency remains high, resulting in high power communication as well as data loss and transmission failure as well as coverage issues and route breakage, among other issues, all of which have a significant impact on EV battery system monitoring [17,18]. The BMS requirements are: -Contactors Requirement -Electromagnetic Interference (EMI) Protection in general, galvanic isolation, and redundancy. Other prerequisites Depending on the application, there may be several other needs and restrictions, including those related to space and system costs, which the BMS must satisfy. For aeronautical applications, for instance, mechanical toughness, weight, and power consumption are crucial characteristics.

An IoT BMS based on LR parameter estimate and an Ormes Net gateway topology is being developed with the long-term goal of improving cost effectiveness, safety, reliability, and optimal operation of large-scale battery energy storage systems. NSFC is financing the project.

Literature survey

A cloud-based framework was developed by an international team of researchers under the direction of Amit Adhikaree and associates [19] for monitoring the condition of Lithium-Ion (Li-ion) battery systems on a wide scale. The platform was created using cloud-based services and Internet of Things (IoT) gadgets. The Internet of Things components featured sensors and actuators in addition to battery-powered wireless data collection and communication devices. These parts allowed modules to communicate both with one another and with the internet. Cloud computing combines elements including cloud storage, analytics software, and visualisation. Based on the results, the cloud was able to use its high-performance computer resources to precisely monitor the battery's status of charge. As a result, the established method increased the operational efficiency and scalability of large-scale battery energy storage systems. It also reduced their cost. Despite the approach's superiority, the coverage problem remained unresolved.

Weihan Li and colleagues [20] developed a cloud-based battery management system for battery systems with the goal of increasing computational power and data storage capacity using cloud computing. Using the Internet of Things, all battery-related data was collected and delivered to a cloud-based storage system. Battery diagnostic algorithms analysed the data and built a digital twin of the battery system therefore to better understand the battery's charge and ageing state. Using cloud-based algorithms to predict battery system state-of-charge and health, the applicability of similar circuit models in digital twin battery systems was examined. An technique that uses particle swarm optimization to assess battery capacity and power fading as it ages was also examined. However, the SOH's evaluation was lowered by the hazy sounds.

T. Taesic Kim and coworkers [21] have created a cloud-based technique for tracking and diagnosing battery faults in big Li-ion battery energy storage systems [21]. [21] (BESS). The built cyber-physical platform comprised a cloud-based platform for regulating the battery modules' performance, which incorporated the Internet of Things into the battery modules. A battery defect diagnostic algorithm based on outlier mining and condition monitoring have been developed for the Cloud Battery Management Platform (CBMP). The CBMP cost analysis and the cyber-physical testbed were utilised to verify the approach. This resulted in intelligent and cost-effective BESS systems and onboard health monitoring for big Li-ion BESS systems. Due to signal transmission's high rate of data loss, the approach was insisted upon.

Mohammad Asaad and colleagues [22] created an optimization model to maximise trade income for EV aggregators using smart charging to boost profitability. To reduce battery degradation, a real-time Battery Monitoring System (BMS), an Enhanced Coulomb Counting Method for SoC estimation, and the messaging-based MQTT communication protocol were provided. To install the new BMS, a hardware platform comprising sensing technology, a central CPU, interface devices, and Node-RED software was designed. Enhanced Coulomb counting considers self-discharge, temperature dependence, and aging-related degradation. Overshoot and poor SOP estimation hampered the approach.

According to Guillaume Le Gall et al. [23], it is possible to use IEEE Std 802.15.4 Time Slotted Channel Hopping, a standardised protocol for low-power, lossy networks, in conjunction with other protocols. Beginning with real-world tests in which the link quality of wireless nodes contained within an electric vehicle battery pack was examined at the Medium Access Control layer, the paper moved on to discuss theoretical considerations. Afterwards, using the findings of the investigations, it developed two topology management strategies and scheduled a method known as Linear Programming and Simple Descent, which are both based on linear programming. Because of battery management constraints, the goal was to achieve effective data transfer while remaining within those constraints. However, the approach was exceedingly complex and prone to multiple interferences.

The remaining parts of the article are structured as described below. The connected works are presented in Section 2. Following that, the following section (section 3) presents a comprehensive examination of the suggested model. Following that, the performance of the suggested model is assessed in part 4, and the investigation is wrapped up in section 5.

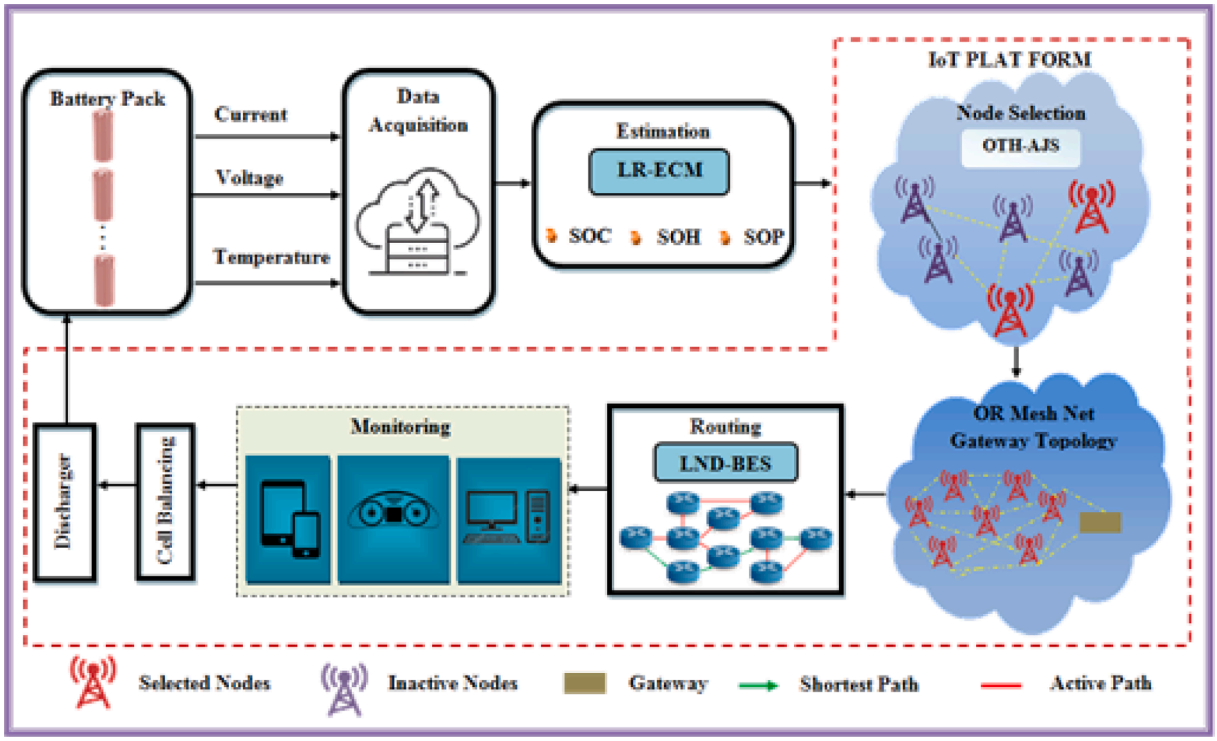

Fig. 1. Proposed IoT BMS Framework.

Proposed IoT BMS framework

Electric vehicle battery management systems ensure the safe operation of the battery pack and communicate this information to other systems. IoT-based BMS monitors the battery online and helps prevent it from running outside of its safe operating range due to issues including excessive current, voltage, undervoltage, and temperature. Due to inaccuracies caused by current sensor or voltage sensor uncertainties as well as the unusual occurrence of relaxation state, open-loop approaches for calculating SOC, SOH, and SOP parameters are less reliable [24]. Monitoring and control, as well as remote data logging for battery attributes, conditions, and other factors, are all significantly aided by the Internet of Things (IoT). The term "Internet of Items" describes a network of actual physical things (things) that have been outfitted with sensors, software, and other technologies to communicate and exchange data with other systems and devices online. Devices with low power consumption and wide coverage are essential for the future of renewable energy. The capacity of a channel diminishes as the bandwidth decreases. Its bandwidth ranges from 20 to 40 MHz, though its ranges from 40 to 100 m, and its power consumption is high. While dormancy is high and IoT links regularly accept postponement, it leads to high power transfer, data loss and transmission failures as well as coverage concerns and poor routing or route breaking that have a substantial influence on battery-operated system monitoring in electric cars. Machine learning and artificial intelligence algorithms are utilised to analyse all battery-related data in real-time, including voltage, current, and temperature readings during charging and discharging. If a problem with the battery is found, the driver or service provider should be contacted [25]. As a result, there is an enhanced likelihood that a battery can be repaired or replaced before it fails or is irreparably damaged. The study has created an IoT BMS based on LR parameter estimate and ORMeshNet gateway topology to address the difficulties at hand, as shown in Fig. 1.

Data acquisition

As many as possible sensors are used to gather data that can be analysed in order to figure out how much charge is being stored in a battery cell at any one point in time. IoT Gateway/router transfers the data from communication component, which is the optimal node for the IoT device. Using the cloud battery management system, the module management system receives health monitoring information and control recommendations from the cloud battery management system. Sensor acquisition systems for Internet of Things devices usually contain a short-range radio, such as Wi-Fi, Zigbee, or low-power Bluetooth. These radios use Internet of Things protocols such Queue Telemetry Transport and Constrained Application Protocols [26] to communicate data and signals to other modules or a concentrator. Additional data aggregation, storage, and analysis are expected to be needed in the future as the Internet of Things Gateway generates huge volumes of information from many sources.

Estimation

Changes in model parameters and the SOH during real-world battery use are well known to have a significant influence on both the SOC and SOP. Ignoring the nature of such interaction, i.e., calculating SOC/SOH/SOP in isolation is likely to reduce battery condition monitoring accuracy and resistance to variations in operational circumstances and health status.

SOC and SOH estimation based on Lasso regularization

One of the most important jobs of a battery management system is to estimate the state of charge (SOC) of the batteries. SOC is the ratio of a battery's current capacity to its maximum nominal capacity. The state of charge, or SOC, is an important measurement for figuring out how well the battery storage systems in electric cars work (EV). Lithium-ion batteries have therefore been actively researched in terms of SOC estimate due to their fast charging, extended life cycle, and high energy density properties [27]. The regression known as the Lasso (least absolute shrinkage and selection operator) decreases the residual sum of squares subject to the absolute value sum. Due to its outstanding performance in both variable selection and prediction accuracy, Lasso is frequently used

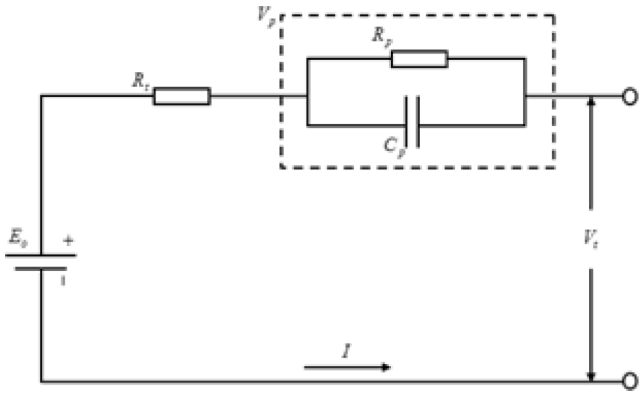

Fig. 2. First-order RC ECM.

to predict continuous variables. Lasso was used by Mansouri et al. to forecast a battery's RUL. As a result of this, Friedman et al. [28] developed fast estimation algorithms for extended linear models with convex penalties. Fig. 2 shows how the dynamic characteristics of the lithium-ion battery can be described using a first-order RC ECM. To symbolise polarisation resistance and capacitance, we'll use Rp and Cpae in Fig. 2, while Rt represents ohm resistance. Predicted terminal voltage, open-circuit voltage (I 0, V 0), and the voltage at which polarisation occurs (V p) are all calculated. SOC and I 0 have a nonlinear connection with respect to one another. The battery is allowed to rest for an hour after attaining SOC before its power characteristics are assessed. The battery's power characteristics are reduced by 10 % each time the battery is allowed to rest; simultaneously, I 0 is measured. Piecewise linear interpolation can be used to obtain the function I 0 = n soc + n.

Assuming the state variables $a = [a_1, a_2]^T = [V_p, soc]^T$ and In accordance with Kirchhoff's voltage law (KCL), the state equation is as follows:

$$a^{'} = Ma + Nu \tag{1}$$

$$S = Pa + Qu \tag{2}$$

Where, $= \begin{bmatrix} 0 & 0 \\ 0 & -1/R_p c_p \end{bmatrix}$,$N = \begin{bmatrix} 1/c_n \\ 1/c_p \end{bmatrix}$, $P = [\alpha_n \quad 1]$, $Q = \quad R_t$, $S = V_t - \beta_n$, $u = i$.

Using the z transform, discrete the Equations (1&2) to yield the Equation (3) as follows:

$$V_t(k) = \alpha_1 . V_t(k-1) - \alpha_2 . V_t(k-2) + \beta_0 . i(k) - \beta_1 . i(k-1) - \beta_2 . i(k-2) \tag{3}$$

Where,α_1, α_2, β_0, β_1, β_2 are the parameters to be estimated.

In existing parameter estimation, the new approximation is equivalent to the sum of the previous estimation, which has a substantial influence on the meeting rate and following presentation. To address this issue, the work employed Lasso regularisation to manage the convergence rate and track the performance. Lasso regularisation employs a penalty constant ((h_1)) to maintain the learning rate (ƛ)) low enough for the method to rapidly track the local trend of non-stationary signals and, in a steady environment, gradually increase to enough to minimise parameter estimate error.

If LR is not done, then when ƛ is equal to 1, all faults are always considered, and the tracking capabilities are inadequate. It is noise-insensitive, and the parameter estimate error in the steady-state is negligible. It is not susceptible to noise, and the error in estimating the steady-state parameters is small [29]. The evaluation of present faults is limited when ƛ is equal to zero, and while the tracking capabilities of time-varying parameters is significant, it is more susceptible to noise when is equal to 0.

The lasso regularization is performed based on the,

$$Y(k) = \Phi^T(k).\Theta \tag{4}$$

$$E(k) = Y(k) - \Phi^T(k).\widehat{\Theta}(k-1) \tag{5}$$

$$L(k) = \min_{\lambda \in R_n} \left\{ \frac{\| Y(k) - \lambda(\Phi^T(k).\widehat{\Theta}(k-1)) \|}{2n} + \hbar \|\lambda\|_1 \right\} \tag{6}$$

Where $E(k)$ is $Y(k)$ the assessed fault,$\Theta = [\alpha_1, \alpha_2, \beta_0, \beta_1, \beta_2]^T L(k)$ is the lasso regularization purpose. Rendering to the planned procedure, we can obtain the moderate value of the estimation parameter using the LR. Now the parameters of the battery system are finded out using the eqn:

$$ocv = \beta_2 \tag{7}$$

$$R_t = \alpha_1 \alpha_2 \tag{8}$$

$$R_p = \frac{\beta_0 - \alpha_1 \alpha_2 \beta_1}{1 + \beta_1} \tag{9}$$

$$c_p = \frac{T_S}{\beta_0 - \alpha_1 \alpha_2 \beta} \tag{10}$$

SOH estimation. The Battery Management System (BMS) must consider the battery's State of Health (SOH) and State of Charge (SOH) in order to prevent battery failure and extend battery longevity (SOH). SOH estimation can tell us how successfully a lithium-ion battery stores and distributes electricity within a power grid. It's a useful tool [30]. The Gaussian process regression with neural network (GPRNN) as its variance function is presented to analyse and forecast battery state of charge. Equation (11), where c n is the nominal capacity of a new cell and represents the capacity that remains after ageing, defines battery SOH. As indicated in Eq., the accumulated charge and the difference in SOC over time can be used to directly attain the current capacity based on the SOC variation (12). (13).

Here, $soc_\alpha = [\alpha_1, \alpha_2]$ and $soc_\beta = [\beta_0, \beta_1, \beta_2]$ are SOC estimates given by LR at the time step α and β, and ΔAH means the ampere-hour accumulation between α and β. The estimated SOC at the headmost time step in the horizon instead of the SOC at the end of the horizon is applied. Considering that the capacity is a slow variable parameter in the aging process, the SOH monitoring is realized offline at a regular interval.

$$soh = \frac{c}{c_n} \tag{11}$$

$$soc_\beta = soc_\alpha - \frac{\Delta AH}{c} \tag{12}$$

$$c = \frac{\Delta AH}{soc_\alpha - soc_\beta} \tag{13}$$

SOP estimation

To describe the greatest amount of electricity that a power battery can continuously release or absorb over a defined time, we use the term "state of charge" (SOP). An essential part of the battery management system is the calculation of SOP, which is required to provide electric vehicles with stable and reliable output power and to assure their safety over a specific period. The SOP indicates how quickly a battery's energy can be added to or removed without violating a set of design limits stated by the manufacturer [31]. First, think about the power restrictions under voltage restrictions. Equation (14) is used to compute the voltage across the RC Network at the present time step k:

$$V_p(k) = OCV - V_e(k) - i_e(k) R_0 \tag{14}$$

Then, its prediction value at the next time step can be derived based on the discretized form of Equation (3), as Equation (15):

$$V_p(k+1) = e^{-\frac{T_S}{R_p c_p}} V_p(k) + \left(1 - e^{-\frac{T_S}{R_p c_p}}\right) R_p i_e(k) \tag{15}$$

Then, the current limits corresponding to the upper and lower voltage limits are calculated as Equation (16):

$$i_e^{discharge}(k+1) = \left[ocv - V_p(k+1) - V_{\min}[]_p\right] \tag{16}$$

Where, V_{max} and V_{min} represent the upper and lower cut-off voltage respectively.

At last, the power limits at discharge and charge conditions are constrained by voltage limits as Equations (17) and (18):

$$sop^V_{discharge} = V^{discharge}_{emin} \tag{17}$$

$$sop^V_{charge} = V^{discharge}_{emax} \tag{18}$$

Then analyse the power limitations imposed by present restrictions. As previously mentioned, the voltage across the RC network at the next time step must first be computed using Equations (14) and (15). Equations (19) and (20) are then used to derive the voltage limitations that correspond to the higher and lower current limits:

$$V_e^{discharge}(k+1) = ocv - V_p(k+1) - R_0 I_{max} \tag{19}$$

$$V_e^{charge}(k+1) = ocv - V_p(k+1) - R_0 I_{min} \tag{20}$$

Where, I_{max} and I_{min} represent the maximum and minimum current, respectively. At last, the power limits at discharge and charge conditions constrained by current limits as Equations (21) and (22):

$$sop^I_{discharge} = I^{discharge}_{emax} \tag{21}$$

$$sop^I_{charge} = I^{discharge}_{emin} \tag{22}$$

Finally, examine the power restrictions imposed by SOC constraints. The polarisation voltage over the RC network must still be calculated using Equations (14) and (15). Equations (23) and (24) may be used to compute the current limitations under SOC constraints:

$$I_{\min}^{soc_n\left[soc(k) - soc_{\min}[]_p\right]} \tag{23}$$

$$I_{\max}^{soc_n\left[soc(k) - soc_{\max}[]_p\right]} \tag{24}$$

Where soc_{max} and soc_{min} indicate the planned upper and lower cut-off SOCs, and T_p signifies the temporal window size, which may be modified to decide when the SOC restriction is activated. For the discharging process, a longer T_p equals lower current restrictions, and hence an earlier triggering of SOC limitations. Because Equations (23) and (24) have translated the SOC constraints to current limitations, the peak power under SOC limitation for the discharging and charging processes (denoted as $sop^{soc}_{discharge}$ and sop^{soc}_{charge} respectively) may be obtained from the same formula under the current constraint [32]. Finally, the battery power will be restricted by the least absolute value of the three limitations indicated above, which means as Equation ((25) & (26)):

$$sop_{discharge} = min\left[sop^V_{discharge}, sop^I_{discharge}, sop^{soc}_{discharge}\right] \tag{25}$$

$$sop_{charge} = min\left[sop^V_{charge}, sop^I_{charge}, sop^{soc}_{charge}\right] \tag{26}$$

Finally, the estimated SOC, SOH, and SOP need to be communicated via the IoT platform. The data estimated gets stored over the optimal IoT nodes and they are transferred via a protocol to manage the Battery of the EV.

Optimal node selection in IoT platform

Communication between Internet of Things (IoT) devices is routed through a variety of networks. The Internet of Things connects all nodes to the Internet by utilising physical products that are equipped with a variety of sophisticated sensors of various types. Many Internets of Things nodes generate and transmit vast volumes of data, simplifying daily life, assisting with challenging decision-making, and offering crucial services to customers. Thus, the Internet of Things is predicted to rapidly develop as one of the most used networking technologies, delivering a wide range of advantages to consumers. However, message delivery latency is still a critical performance metric that should be minimised to the absolute minimum. As a first step toward addressing the issues, the team used an Artificial Jellyfish Search based on Optimal Tuning Hyperparameters to pick nodes for further investigation (OTH-AJS). An approach to node selection has been developed using jellyfish searching behaviour in ocean currents. This behaviour comprises amazing mechanisms including their convergence into jellyfish blooms, a time control mechanism for switching between different movements, and their movement inside a jellyfish swarm (active and passive motions). The jellyfish search (JS) algorithm optimises by observing jellyfish activity in the water. Published in 2021 by Jui-Sheng Chou et. Jellyfish can move freely. Regardless, they usually drift with the tides. A jellyfish bloom is a large swarm of jellyfish. Conditions such as temperature and ocean currents influence swarm formation. The most important factor is swarming jellyfish. As a result, jellyfish can be found almost any place in the ocean. Because meal amounts vary, comparing food proportions would indicate the ideal position. So we developed a new algorithm based on jellyfish search and movement in the ocean [33]. Jellyfish optimizer. This method aids in the search for and selection of the optimum node for storing measurements. However, the high computational complexity, poor balance of exploitation and exploration rates, and low convergence rate result in a significant error rate when selecting the best nodes. The work uses an OTH-AJS optimizer to solve this problem. The proposed method employs Normalized Xavier Initialization of the jellyfish position in exploitation phased mode and regulates the balancing rate. The method additionally addresses on computing complexity and the convergence rate problem by employing a Bit shift map for jellyfish population initialization.

Based on the features of the node the optimal node gets selected. The node features (F_{Nodes}) used are residual energy of the nodes (N_{res}), proximity (N_{prox}), distance to the user (N_{db}), cost (N_{cost}), and node centrality or coverage (N_{cov}), etc. The objective of selecting the node is given by taking a weighted sum approach ($\Re_i$) for different features and forming into one scalar objective function given as:

Academics and industry are interested in the Internet of Things (IoT) as a new technology. An Internet of Things node is a small gadget powered by batteries. The data collected by IoT nodes will be routed through a gateway server, which will combine it and send it to a cloud platform for further processing. When IoT nodes are dispersed across a large area, nodes located far from the gateway server must transport data across many hops to the gateway server. To optimise power usage and maximise node operational time, the next forwarding node might be chosen based on the greatest power level available among numerous candidate nodes [34]. The ideal node is chosen based on the node's characteristics. The node characteristics (F_{Nodes}) employed include residual energy (N_{res}), proximity (N_{prox}), distance to the user (N_{db}), cost (N_{cost}), and node centrality or coverage (N_{cov}), among others. The goal of picking the node is done by using a weighted sum technique ($\Re_i$) for multiple attributes and combining them into a single scalar objective function. As a result, the Internet of Things is predicted to swiftly ascend to one of the most widely used networking technologies, giving a variety of benefits to consumers. Even though the nodes in these networks are frequently delay-tolerant, message delivery latency is a critical performance indicator that should be kept to a minimum.

$$\Omega\left((F_{Nodes}) = \max_{\Gamma}[\Gamma_1 N_1 + \Gamma_2 N_2 + \Gamma_3 N_3 + \Gamma_4 N_4 + \ldots\ldots + \Gamma_n N_n]\right) \tag{27}$$

Input: Node features $\left(F_{Nodes}\right)$

Output: Optimal Nodes

Begin

Initialize the objective function

$$\Omega\left(\left(F_{Nodes}\right)\right)=\max_{\Gamma}\left[\Gamma_1 N_1+\Gamma_2 N_2+\Gamma_3 N_3+\Gamma_4 N_4+.....+\Gamma_n N_n\right]$$

For i in F_{pop}

Calculate time control

$$\mathrm{T}(t)=\left|\left(1-\frac{t}{\max_{iter}}\right)\times\left(2\times rand(0,1)-1\right)\right|$$

IF $\mathrm{T}(t)\geq 0.5$

Compute functioning mechanism of ocean current using,

$$\Omega=\frac{1}{F_{pop}}\sum\Omega_i=\frac{1}{F_{pop}}\sum\left(N-\aleph_e N_i\right)=N-\aleph_e\frac{\sum N_i}{F_{pop}}=N-\aleph_e\upsilon$$

Compute the new position of the jelly fish

$$N_i(t+1)=N_i(t)+rand(0,1)\times(N_i^*-D_{\mathcal{C}}\times rand(0,1)\times\upsilon)$$

Else

Return jellyfish inside swarm

If $rand(0,1)>\left(1-T(t)\right.$

Compute Type A motion

$$N_i(t+1)=N_i(t)+\nu\times rand(0,1)\times(U_B-L_B)$$

Else

Compute type B motion

$$N_i(t+1)=N_i(t)+SP$$

$$SP=NXI\left(-\frac{\sqrt{6}}{\sqrt{N_i(t-1)+N_i(t)}},\frac{\sqrt{6}}{\sqrt{N_i(t-1)+N_i(t)}}\right)\times dir$$

End if

End if

Check the Boundary Condition

Finally update the best position,

$$\begin{cases}N''_{i,d}=(N_{i,d}-U_{B,d})+L_B(d) & ifN_{i,d}>U_{B,d}\\ N''_{i,d}=(N_{i,d}-L_{B,d})+U_B(d) & ifN_{i,d}>L_{B,d}\end{cases}$$

End for

Obtain the optimal node

End begin

Fig. 3. Pseudo code for OTH-AJS.

To limit the amount of food available to the jellyfish, the selection is dependent on the way in which they function (the fitness value of their nodes). The current best answer is to follow all of the jellyfish's paths in the same direction as the sea current. Following is the formula for ocean currents.

$$\Omega=\frac{1}{F_{pop}}\sum\Omega_i=\frac{1}{F_{pop}}\sum(N-\aleph_c N_i)=N-\aleph_c\frac{\sum N_i}{F_{pop}}=N-\aleph_c\upsilon \tag{28}$$

$$df=\aleph_c\upsilon \tag{29}$$

Where F pop denotes the jellyfish population; Ni is the jellyfish that currently has the best placement in the swarm; ℵ_c is the attraction factor; is the average location of all jellyfish; df is the difference between the jellyfish's current best location and the average location of all jellyfish.

During the spatial distribution, a distance about the mean place covers some probability of entirely jellyfish, that is

$$df=\wp\times\phi\times rand^f(0,1) \tag{30}$$

$$\phi=rand^{\alpha}(0,1)\times\upsilon \tag{31}$$

Where, ϕ is the standard deviation of the distribution.

The new location of each jellyfish is now provided by the jellyfish locator:

$$N_i(t+1)=N_i(t)+rand(0,1)\times\left(N_i^*-D_C\times rand(0,1)\times\upsilon\right) \tag{32}$$

Where, $D_C>0$ is a distribution coefficient related to the length of ϕ.

The motion of the jellyfish is constrained within two groups, and they are Type-A motion and Type-B gesture. In addition to specifying the type-A motion of jellyfish around their own locations, the updated location of each jellyfish is also supplied.

$$N_i(t+1) = N_i(t) + \nu \times rand(0,1) \times (U_B - L_B) \tag{33}$$

Where U_B and L_B denotes the upper and lower bounds of search areas.

$\nu > 0$ is a motion coefficient related to the length of motion around jellyfish's locations.

According to the Type B motion, a jellyfish is picked at random, and then the motion is estimated along the direction of food based on the amount of food and change in the jellyfish's position. This motion is known as a propagating motion. After that, the current position of the exploitation is brought up to date by employing,

$$N_i(t+1) = N_i(t) + SP \tag{34}$$

$$SP = NXI\left(-\frac{\sqrt{6}}{\sqrt{N_i(t-1) + N_i(t)}}, \frac{\sqrt{6}}{\sqrt{N_i(t-1) + N_i(t)}} \right) \times dir \tag{35}$$

$$dir = \begin{cases} N_j(t) - N_i(t) iff(N_i) \geq f(N_j) \\ N_i(t) - N_j(t) iff(N_i) < f(N_j) \end{cases} \tag{36}$$

Where, *NXI* denotes the normalized Xavier initialization, $N_i(t-1)$ represents the previous position of the jellyfish.

The type of motion that has taken place throughout time is detected using a time control system. Type A and type B motions inside a swarm, as well as jellyfish movement along a water current, are all controlled by this system. Over the duration of a particular time, the time control function generates a random number between 0 and 1.

$$\mathrm{T}(t) = \left| \left(1 - \frac{t}{max_{iter}}\right) \times (2 \times rand(0,1) - 1) \right| \tag{37}$$

Where t denotes the time supplied as the iteration number and max_iter is an initialised parameter denoting the maximum number of iterations.

Randomly priming the jellyfish population causes delayed convergence and traps it at local minima. The work has employed a bit-shift map to increase convergence speed. Compared to random selection, this map produces more diversified starting populations and decreases the likelihood of premature convergence. The bit shift mapping is formulated as within the range of $\forall : [0,1) \rightarrow [0,1)^{\infty}$ where $\forall = [Z_1, Z_2, Z_3, ...Z_n]$, and initially,$Z_0 = Z$. Now, the iterated function of the mapping is given as:

$$N(x) = \begin{cases} 2x & 0 \leq x \leq \frac{1}{2} \\ 2x - 1 & \frac{1}{2} \leq x < 1 \end{cases} \tag{38}$$

Shifting one bit to the right and replacing one "one" with a "zero" is how an iteration's value is calculated if it is stated in binary notation, as seen in this example.

Certain conditions are followed by the jellyfish that is when the jellyfish returns after circulating over the entire oceans, the efficient position of the jellyfish is assumed by:

$$\begin{cases} N''_{i,d} = \left(N_{i,d} - U_{B,d}\right) + L_B(d) if N_{i,d} > U_{B,d} \\ N''_{i,d} = \left(N_{i,d} - L_{B,d}\right) + U_B(d) if N_{i,d} > L_{B,d} \end{cases} \tag{39}$$

Where, $N_{i,d}$ is the location of the i^{th} jellyfish in d^{th} dimension; $N''_{i,d}$ is the effectual position subsequently examination border restraints. Finally based on the boundary conditions the fitness of the nodes is evaluated and the best values are selected and through which the data are stored and transferred to the IoT gateway. Thus, the overall outline of the proposed OTH-AJS is illustrated in the form of pseudo code in Fig. 3.

IoT gateway protocol

The parameters obtained by the gateway are transmitted to the node. The primary function of a gateway is to transfer data packets over a network from end devices to a primary server, typically over a backhaul interface, radio link, or 3G or 4G wireless network connection. IoT mesh nodes provide more intriguing regulations for connecting a range of networks and radio technologies, and so completely fulfil the ever-increasing demands of subscribers such as mobility, Quality of Service (QoS), and security. On the other hand, mesh architecture enables devices to communicate with other network nodes (i.e., point-to-multipoint connections) via a capability known as multi-hopping [35]. A message can "hop" from one node to the next until it reaches its intended recipient. Mesh topology has a lot of advantages over star topology, including a greater range distance and less data or transmission loss. However, without knowledge of the connections between network nodes, as well as their channel width for a given frequency range for data transfer, this may result in high power communication, coverage issues, poor routing, transmission failure, data loss, route breakage, and other issues that have a significant impact on battery monitoring. To address this issue, the team created an Optimal Routing Mesh networking (ORMeshNet) gateway topology.

Consider the ideal node set $N = [n_1, n_2, ...n_n]$ and L is the set of feasible direct communication lines. Each node $n_i \in N$ represents an access point (AP) with a circular transmission range T_R and an interference range I_R. Among the total number of wireless nodes N, some are gateways that link to the Internet. Consider the set of m gateway nodes $G = \{g_1, g_2, ...g_m\}$, where g_i is the node for n_{n+i-m} ,for $1 \leq i \leq m$. All of the other wireless nodes $n_i\,(1 \leq i \leq n-m) \in N \backslash G$ are standard mesh nodes.

Each regular mesh node receives traffic from all of its connected users and routes it to the Internet via some gateway nodes. We assume that each node $n_i \in N$ has a limited capacity to serve its associated data, which is represented by D_i, but that the capacity between any gateway nodes to the Internet (to send its incoming traffic to the Internet) is adequate.

During the transmission of the node $n_i \in N$, all nodes within its transmission range, and therefore representing its neighbourhood represented by $\forall_e(i)$, get the signal from n_i with sufficient power to allow for proper decoding with a high probability. It should be emphasised that transmitting data without knowing the connections between network nodes, as well as their channel width for a specific frequency range, might result in significant data loss. Optimal routing is produced using Bald Eagle search optimization, which takes into account energy and throughput optimization issues [36]. Various optimization limitations are taken into account, including connection capacity restrictions, flow conversations, flow conversations at the gateway, interference constraints, and so on.

The objective function to be reduced is shown in the equation, and it consists of lowering the network's energy consumption while maximising network throughput throughout the considered period t. The goal is to create a new routing protocol that can locate ways across a network while captivating into consideration trade-offs such as energy usage and throughput, such as:

$$min \frac{\zeta \ell + (1-\zeta) N \Re}{t} \tag{40}$$

Where 0 is a weighting coefficient that is used to balance the amount of energy consumed and the rate of consumption. If $= 0$, we are primarily concerned with increasing the rate that can be achieved, and if $= 1$, we are concerned with reducing energy use while increasing throughput. In order to obtain optimal weighing coefficient for finding out the optimal route with balanced energy and throughput trade-offs, the work has developed a Logit Normal Distribution based BES optimizer (LND-BES). The developed technique for optimal routing performs a faster convergence rate and maintains the search pattern between local and global points which tends to achieve an accurate routing with low computational complexity. The Logit normal distribution is used instead of random updating to update the final position of the best eagle during the

swooping stage. The logit normal distribution analyses the spread of the prey and finds out the closest best solution to attain the convergence.

The best approach is determined by bald eagles' hunting method or sophisticated social behaviour when searching for fish. The bald eagles (weighting coefficient) identify and pick the optimal location in terms of the quantity of food (route) inside the designated exploration space (constraints) where they may look for prey in the first stage of the procedure. Equation (41) is a mathematical representation of this behaviour.

$$\zeta_{new}, i = \zeta_{best} + \nu^{*} l(\zeta_{mean} - \zeta_i) \tag{41}$$

As for the positional parameter, it has a range of values from 1.5 to 2 and is a random integer between 0 and 1. They choose where to build their nest after gathering all the information they need from the previous stage. This is referred to as the "selecting step." The eagles choose a new area for their search, but it is still within a reasonable distance. That which is now being searched for by bald eagles in this case is called "best" because it was found in their most recent search. In the previously selected search region, the eagles fly through the area at random. Meanwhile, the ζ_mean indicates that these eagles have devoured all the information contained in the previous points.

By multiplying the randomly searched earlier information by ν, the present movement of bald eagles may be calculated. All search points are changed at random during this procedure.

To speed up their search for prey, the birds then fly in different directions within a spiral space to further narrow their search area. When it comes to calculating the ideal swoop position, Eq. (42).

$$\zeta_{i,new} = \zeta_i + p(i)^{*}(\zeta_i - \zeta_{i+1}) + q(i)^{*}(\zeta_i - \zeta_{mean}) \tag{42}$$

$$q(i) = \frac{ql(i)}{max(|ql|)}, p(i) = \frac{pl(i)}{max(|pl|)} \tag{43}$$

$$ql(i) = l(i)^{*}sin(\theta(i)), pl(i) = l(i)^{*}cos(\theta(i)) \tag{44}$$

$$\theta(i) = z^{*}\pi^{*}rand \tag{45}$$

$$l(i) = \theta(i) + W^{*}Rand \tag{46}$$

W, an integer with a value between 5 and 10, controls the number of corner-to-corner point searches in the centre point, and z, a parameter, controls the number of search cycles in the centre point.

The bald eagles then go on to the swooping stage, where they swing from the best position in the search space to their prey. All points are also moving in the direction of the best point. This behaviour is quantitatively shown in Equation (47).

$$\zeta_{i,new} = F + \zeta_{best} + ql(i)^{*}(\zeta_i - c_1{}^{*}\zeta_{mean}) + pl(i)^{*}(\zeta_i - c_2{}^{*}\zeta_{best}) \tag{47}$$

$$F(\zeta_{best} : \eta, \sigma) = \frac{1}{\sigma\sqrt{2\pi}} \frac{1}{\zeta_{best}(1-\zeta_{best})} e^{-\frac{(logit(\zeta)-\eta)^2}{2\sigma^2}} \tag{48}$$

Where$c_1 c_2 \in [1, 2]$, $F(\zeta_{best} : \eta, \sigma)$ denotes the Logit normal distribution of the best solution by considering mean η and standard deviation σ. Eagles' motions take on a variety of forms. Polar equations describe the swooping action of these eagles. It is also necessary to consider both the difference between the current and best points and the difference between those two points while trying to figure out where the best point should be on the y-axis. Considering that the parameters c 1 and c 2 increase the intensity of movement of bald eagles toward the best and centre places, the best solution must be multiplied by a random integer to obtain the result. Using the best answer as a starting point, the objective function can be utilised to determine the optimal course of action.

Cell balancing

By maximising the capacity of several series-connected cells and guaranteeing that all of the energy is usable, cell complimentary is a technique for extending the life of a battery pack. The first cell to discharge is also this one. The pack can't reach its full potential as a result. The cell balancing algorithm steps in to help in these situations. Active and passive cell balance are the two different categories of cell balancing strategies. In the active balancing process, which equalises the potential of the cells, the stronger cells are used to charge the weaker cells. By coupling the stronger cells to a load during passive balancing, the excess voltage in the stronger cells is discharged.

Table 1
Evaluation of proposed ORMeshNet with RMSE and TIME metrics.

Estimation/technique	EKF	AEKF	MHE	UKF	Proposed LR
RMSE (%)	0.84	0.84	0.82	0.79	0.35
TIME(s)	0.029	0.025	0.021	0.019	0.009

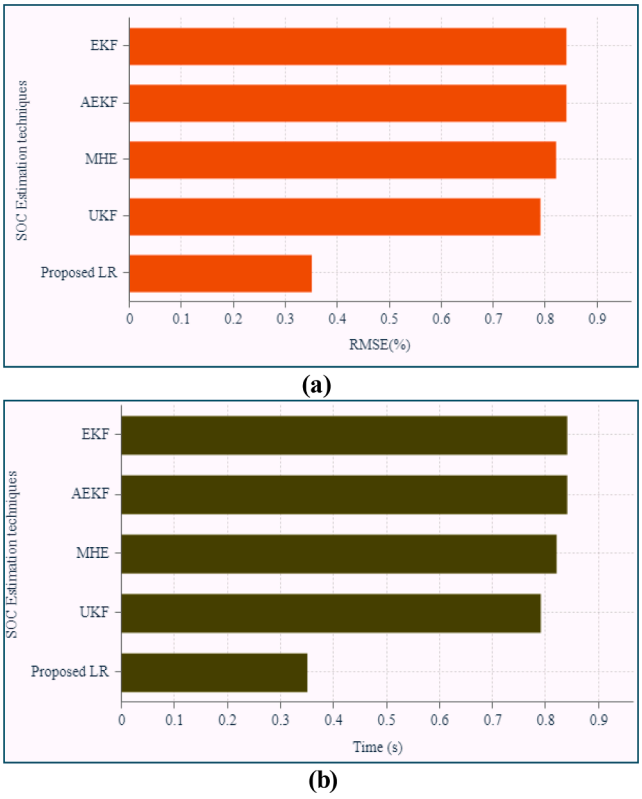

Fig. 4. SOC estimation based on (a) RMSE (b) Time.

Results and discussion

The testing bench is set up for the IoT-based validation of the planned BMS and consists of sensors, a battery testing system, a controller, an ESP8266, and a monitor. The Neware BTS 4000 battery testing system has a maximum current and voltage capacity of 100 A and 5 V, respectively. The data was captured at 1 Hz, and the current and voltage sensors had respective accuracy margins of +0.1 percent and −0.1 percent of the full scale. The scientists examined a cylindrical, 3.35 Ah-capable commercial Li-ion battery (Panasonic NCR18650B). Using high-precision current measurements and a known initial SOC, the coulomb counting method, which has a track record of success, was used to compute the reference SOC. All estimation computations are carried out in MATLAB R2016b on a computer with a 2.30 GHz processor and 8 GB of RAM following the collecting of experimental data.

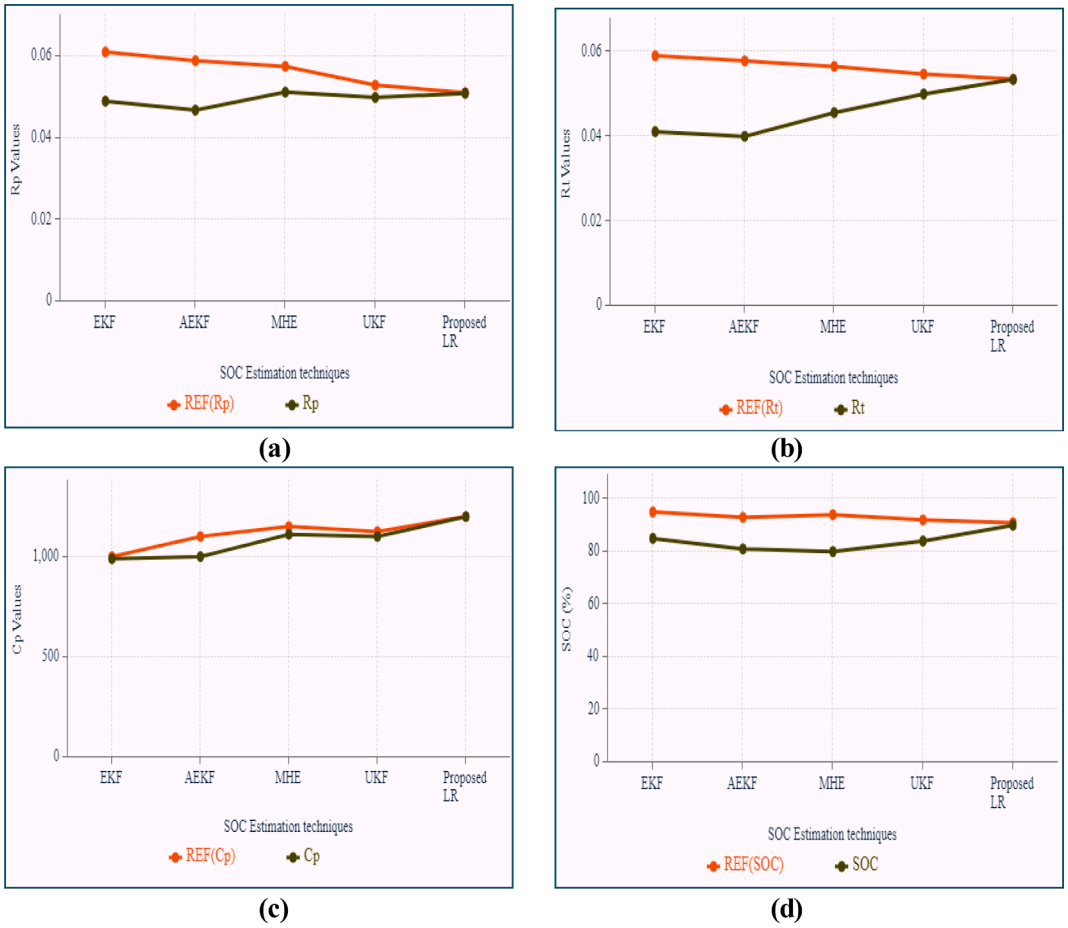

Fig. 5. Estimation of parameters and SOC (a) R_p (b) R_t (c) C_p (d) SOC.

RMSE of SOC estimation and average computational time per step

The root mean square value and time taken for the estimation of SOC by the Proposed LR method is validated against the existing estimation methods such as Extended Kalman Filter (EKF), Adaptive Extended Kalman filter (AEKF), Moving horizon estimation (MHE), and Unscented Kalman filtering (UKF). The values are tabulated in Table 1.

From the above table, it can be illustrated that the proposed LR method tends to estimate the SOC of the battery with low estimation error by achieving an RMSE of 0.35 % and the computation time taken to evaluate the SOC was also low i.e. 0.009 s. But the existing methodologies tend to achieve an RMSE value that is relatively higher as compared to the proposed method i.e. ranging between 0.79 % and 0.84 %. In addition to it, the computing time is also very high i.e. between the ranges of 0.019 s–0.029 s. The lower estimation error and low computing time of the proposed estimation approach are due to the highly efficient parameter estimation by the LR method. The graphical analysis of the proposed estimation of SOC against the existing method is stated in Fig. 1.

Fig. 4 graphically enhances the efficiency of the proposed against the existing estimation methods. It can be stated that the existing methods get badly affected due to overshoot, noises, and other interference that degrades the estimation and leads to a lower performance rate as compared to the proposed method.

SOC estimation outcome

The parameter estimation of the SOC by the proposed LR method is contrasted against the existing methods. The analysis in Fig. 5 is done based on the reference points considered for each parameter.

From the above, it can be said that there is a minute gap obtained between the parameters estimation of the proposed LR method and the reference value for the time ranging between 1000 and 5000 s. The estimation of the SOC parameters by the proposed method remains to be closest to the reference point that is the proposed LR obtains a Polarised resistance of 0.0511 O ~ 0.0509 O, Ohm resistance of 0.0535 O ~ 0.0534 O, the polarised capacitance of 1200F ~ 1199F, and SOC of 91 % ~89.99 %. However, the current technique produces a large disparity between the estimation and the reference position. When calculating the SOC parameter, the present technique trails the reference point by a moderate margin. The moderate margin is owing to poor sensor malfunction and external disturbance management. As a result, as compared to previous approaches, the estimate of SOC parameters is improved.

SOH estimation outcome

To demonstrate the proposed SOH estimator's accuracy and flexibility, Fig. 6 depicts the SOH estimation results with and without noise.

In order to better demonstrate the accuracy of the SOH estimator, Fig. 6 gives out the corresponding graphical analysis. It can be seen that the validation of the battery voltage estimation by the proposed method gives out a small lead of 0.095 V among the reference and estimated voltage and tends to achieve an absolute voltage error of 0.078 V for all battery states under working conditions. The average absolute voltage errors for the proposed method are 1.98 V respectively, which verifies that the proposed method has desirable accuracy and adaptability performance against different loading profiles under all degradation levels. In addition, considering the slow-varying characteristic of capacity decrease, the SOH estimator does not need to be implemented online. It can be triggered every month offline to calibrate the capacity when the BMS is relatively free. Accurate SOH estimation provides the following

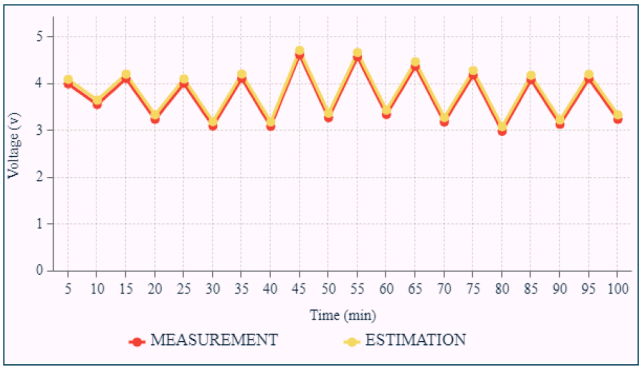

(a)

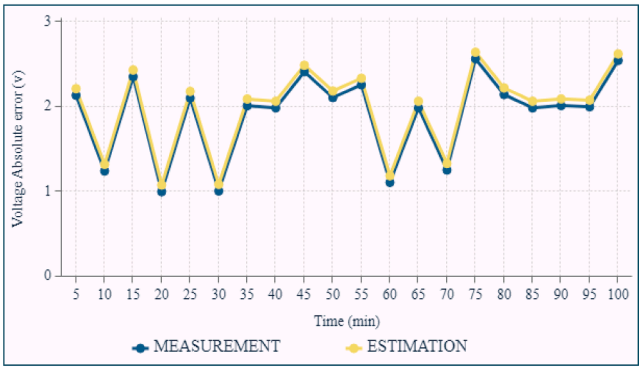

(b)

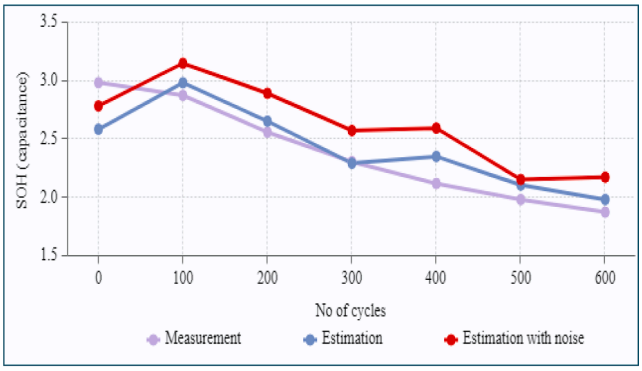

(c)

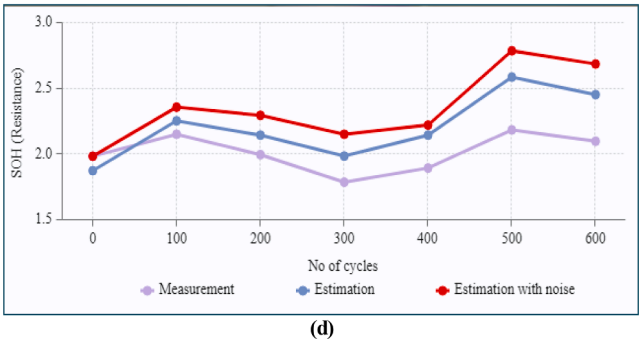

(d)

Fig. 6. Validation of the proposed estimated SOH algorithm based on (a) Validation of battery voltage estimation using LR-calculated parameters and (b) Validation of the suggested estimated SOH algorithm based on When utilising LR-calculated parameters, the absolute error of voltage estimation is computed as follows: SOH(C) concentration measurements and estimations with and without sensor noise are included in this section (d) In the presence and absence of sensor noise, measurements and estimations of SOH(R) are performed.

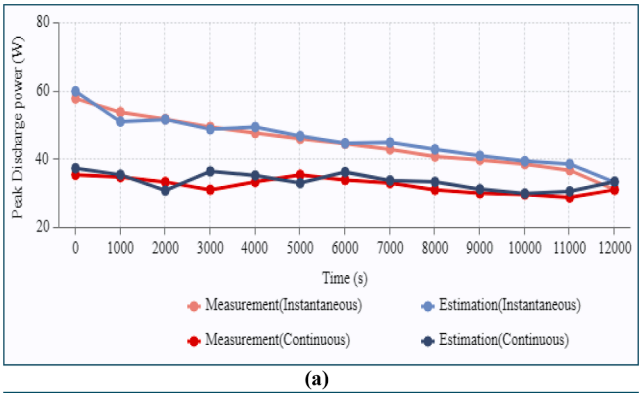

(a)

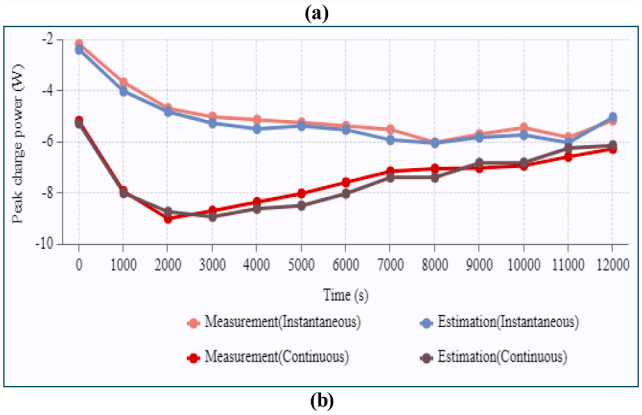

(b)

Fig. 7. SOP estimation (a) Peak discharge power (b) Peak charge power.

SOC and SOP estimators with good estimation bases. Now considering the estimation of SOH for capacitance the proposed method achieves an estimated capacitance difference of 0.036Ah without noise and 0.195 Ah with noise for an average measurement of 2.39 Ah and in terms of SOH for resistance the proposed method achieves an estimated resistance difference of 0.192 V without noise and 0.148 V with noise for an average measurement of 2.016 V. Thus, overall the proposed method tends to be highly adaptive and accurate for estimating the SOH parameters.

SOP estimation outcome

The changes of resistance and capacity degradation during battery operations are considered in the SOP estimation. The maximum discharging and charging capabilities can be obtained by multiplying the measured current by the threshold value of the battery voltage. Based on the measured value, the estimation outcome of the SOP is analyzed in Fig. 7.

From the figure, it can be stated that SOP estimation at peak discharge power tends to be 45.77 W for instantaneous load current and 33.80 W for continuous current. As the respective measurement value is 44.89 W and 32.57 W. It can be stated that for both continuous and instantaneous current the estimated peak discharge power remains to be closer to the measured value which indicates a low absolute error among the estimation of SOC and SOH which enhances the performance of determining the power. In the same manner SOP estimation at peak, charge power tends to be −5.15 W for instantaneous load current and −7.416 W for continuous current. As the respective measurement value is −4.96 W and −5.15 W. The proposed LR is capable to maintain a small SOP estimation error when current and voltage limitations dominate the SOP value at a higher SOC range.

Performance analysis of proposed ORMeshNet gateway protocol

The performance of the proposed IoT gateway protocol is evaluated

based on various metrics such as throughput, PDR, and Goodput in order to analyze the transfer of measured battery data to perform the monitoring and respective control measures i.e. cell balancing.

The proposed gateway network that is ORMeshNet is validated based on throughput, PDR, and Goodput metrics. The validation illustrates that compared to existing methods, such as LoRa, Mesh topology, and Star topology, the proposed method tends to perform better data transfer with less informative data loss. It can be said that data loss was obtained less for the proposed method as it avoids data traffic and also consumes low power to transfer the data, which avoids node failure. Hence, the proposed method achieves a throughput of 88.97 %, PDR of 87.98 %, and Goodput of 83.98 %, whereas the existing methods achieve an overall metrics value ranging between 73.69 % and 79 %, which is relatively less as compared to the proposed method.

Conclusion

An electric vehicle's Battery Management System is a system that ensures the battery pack's safe functioning and reports its status to other systems. IoT-enabled BMS improves battery system monitoring, allowing for more efficient EV operation. Due to many problems such as inadequate calculation of SOC, SOH, and SOP parameters, high data loss, high message delivery delay, and so on, implementing IoT for BMS remains a difficulty. To address this issue the work has developed an IoT BMS based on LR parameter estimation and ORMeshNet gateway topology. The developed work estimates the parameters in a relatively long timescale by improving the accuracy of SOC and voltage estimates as compared to an estimation scheme in isolation. The microelectronic implementation of such a sensor is problematic, particularly for high current and voltage applications; this is one of the few key limitations, which also includes the high cost of implementation. Additional study is required to address these and other issues. In addition, the plan was validated by testing it with lead–acid batteries; however, it still needs to be validated with other common battery types, such as LIBs. The method employs an IoT-optimized routing protocol that optimises the network's channel and frequency resources for resource allocation, such as data storage and transport. The technique shortens the duration of data transmission, guards against data loss or route failure, and manages node failure. Overall, the experimental analysis revealed that the estimated SOH had an absolute error of 1.98 percent, and the calculated SOC obtained an RMSE or estimation error of 0.35 percent. The method transported the data with a throughput of 88.97 %, PDR of 87.98 %, and Goodput of 83.98 % and estimated SOP with a comparatively low error. Finally, when compared to current state-of-the-art techniques, the developed IoT BMS continues to be reliable. The system can be enhanced further by the addition of new functions. By developing a smartphone application that enables users to check their batteries and receive alerts when they are ready to run out of power, the technology can be integrated into cell phones. The internet connection should be improved.

Declaration of Competing Interest

The authors declare that they have no known competing financial interests or personal relationships that could have appeared to influence the work reported in this paper.

Data availability

No data was used for the research described in the article.

References

[1] Tasnimun Faika, Taesic Kim, Maleq Khan, "An internet of things (IoT)-based network for dispersed and decentralized wireless battery management systems", IEEE Transportation Electrification Conference and Expo (ITEC), 13-15 June 2018, Long Beach, CA, USA, 2018.

[2] Lopez AB, Vatanparvar K, Nath APD, Yang S, Bhunia S, Al Faruque MA. A security perspective on battery systems of the internet of things. J Hardware Syst Security 2017;1:188–99.

[3] Sivaraman P, Sharmeela C, "IoT-based battery management system for hybrid electric vehicle", Scrivener Publishing LLC, 1st Edition, ISBN: 9781119681908, 2020.

[4] Vishnu K, Nema RK, Amit Ojha, "Various types of wireless battery management system in EV", IEEE International Students' Conference on Electrical, Electronics and Computer Science, 22-23 Feb 2020, Bhopal, India, 2020.

[5] Hossain Lipu MS, Hannan MA, Tahia FK, Aini H, Mohamad HS, Afida A, Sazal MM, Indra Mahlia TM. Intelligent algorithms and control strategies for battery management system in electric vehicles progress, challenges and future outlook. J Cleaner Prod 2021;292:1–27.

[6] Lucian Andrei Perişoara, Ionuț Constantin Guran, Dumitrel Catalin Costache, "A passive battery management system for fast balancing of four LiFePO4 Cells", 24th International Symposium for Design and Technology in Electronic Packaging (SIITME), 25-28 Oct 2018, Iasi, Romania, 2018.

[7] Mohammadi F, Rashidzadeh R. An overview of IoT-enabled monitoring and control systems for electric vehicles. IEEE Instrum Meas Mag 2021;24(3):91–7.

[8] Ravi R, Surendra U. Charge and health status estimation of a lithium ion battery in an electric vehicle using cell balancing IoT modelling techniques. Int J Chem Chem Eng Syst 2021;6:52–60.

[9] Satpathy S, Mohan P, Das S, Debbarma S. A new healthcare diagnosis system using an IoT-based fuzzy classifier with FPGA. J Supercomput 2020;76(8):5849–61.

[10] Wang X, Xu J, Zhao Y. Wavelet based denoising for the estimation of the state of charge for lithium-ion batteries. Energies 2018;11(5):1–13.

[11] Zhang T, Guo N, Sun X, Fan J, Yang N, Song J, et al. A systematic framework for state of charge, state of health and state of power co-estimation of lithium-ion battery in electric vehicles. Sustainability 2021;13(9):1–19.

[12] Hannan MA, Hoque MM, Hussain A, Yusof Y, Ker PJ. State-of-the-art and energy management system of lithiumion batteries in electric vehicle applications issues and recommendations. IEEE Access 2018;6:19362–78.

[13] Ali MU, Zafar A, Nengroo SH, Hussain S, Junaid Alvi M, Kim H-J. Towards a smarter battery management system for electric vehicle applications a critical review of lithium-ion battery state of charge estimation. Energies 2019;12(3):1–35.

[14] Corno M, Pozzato G. Active adaptive battery aging management for electric vehicles. IEEE Trans Veh Technol 2020;69(1):258–69.

[15] Vaideeswaran V, Bhuvanesh S, Devasena M, "Battery management systems for electric vehicles using lithium ion batteries", Innovations in Power and Advanced Computing Technologies (i-PACT), Innovations in Power and Advanced Computing Technologies (i-PACT), 22-23 March 2019, Vellore, India, 2019.

[16] Morello R, Di Rienzo R, Roncella R, Saletti R, Schwarz R, Lorentz VRH, Hoedemaekers ERG, Rosca B, Baronti F, "Advances in li-ion battery management for electric vehicles", 44th Annual Conference of the IEEE Industrial Electronics Society, 21-23 Oct 2018, Washington, DC, USA, 2018.

[17] Sreedhar R, Karunanithi K. Design, simulation analysis of universal battery management system for EV applications. Mater Today Proc (In Press) 2021. https://doi.org/10.1016/j.matpr.2020.12.136.

[18] Lin Q, Wang J, Xiong R, Shen W, He H. Towards a smarter battery management system a critical review on optimal charging methods of lithium ion batteries. Energy 2019;183:220–34.

[19] Amit Adhikaree, Taesic Kim, Jitendra Vagdoda, Ason Ochoa, Patrick J. Hernandez, Young Lee, "Cloud-based battery condition monitoring platform for large-scale lithium-ion battery energy storage systems using internet-of-things (IoT)", IEEE Energy Conversion Congress and Exposition (ECCE), 1-5 Oct. 2017, Cincinnati, OH, USA, 2017.

[20] Li W, Rentemeister M, Badeda J, Jost D, Schulte D, Uwe Sauer D. Digital twin for battery systems cloud battery management system with online state-of-charge and state-of-health estimation. J Storage Mater 2020;30(1–2):1–12.

[21] Kim T, Makwana D, Adhikaree A, Vagdoda JS, Lee Y. Cloud-based battery condition monitoring and fault diagnosis platform for large-scale lithium-Ion battery energy storage systems. Energies 2018;11(1):1–15.

[22] Asaad M, Ahmad F, Alam MS, Rafat Y. IoT enabled monitoring of an optimized electric vehicle's battery system. Mobile Networks Appl 2017;23(6):994–1005.

[23] Le Gall G, Montavont N, Papadopoulos GZ. IoT network management within the electric vehicle battery management system. J Signal Process Systms 2021. https://doi.org/10.1007/s11265-021-01670-2.

[24] Geetha BT, Santhosh Kumar P, Sathya Bama B, Dutta C, Vijendra Babu D. Green energy aware and cluster-based communication for future load prediction in IoT. Sustain Energy Technol Assess 2022;52:102244. https://doi.org/10.1016/j.seta.2022.102244.

[25] Parthiban S, Harshavardhan A, Prashanthi V, Alhassan Alolo A-RA, Velmurugan S. Chaotic Salp swarm optimization-based energy-aware VMP technique for cloud data centers. Comput Intell Neurosci 2022;2022:1–9. https://doi.org/10.1155/2022/4343476.

[26] Perumal SK, Kallimani JS, Ulaganathan S, Bhargava S, Meckanizi S. Controlling energy aware clustering and multihop routing protocol for IoT assisted wireless sensor networks. Concurrency Computat Pract Exper 2022:e7106. https://doi.org/10.1002/cpe.710.

[27] Mohan P, Alotaibi Y, Alghamdi S, Khalaf OI. An efficient metaheuristic-based clustering with routing protocol for underwater wireless sensor networks. *Sensors* 2022;22(2):415. https://doi.org/10.3390/s22020415.

[28] Jain DK, Tyagi SKS, Prakash M, Natrayan L. Metaheuristic optimization-based resource allocation technique for Cybertwin-Driven 6G on IoE environment. IEEE Trans Ind Inf 2022;18(7):4884–92. https://doi.org/10.1109/TII.2021.3138915.

[29] Asha P, Natrayan L, Geetha BT, Rene Beulah J, Sumathy R, Varalakshmi G, et al. IoT enabled environmental toxicology for air pollution monitoring using AI techniques. Environ Res 2022;205:112574. https://doi.org/10.1016/j.envres.2021.112574.
[30] Berlin S, Tripathi MA, S., et al. IoT-based traffic prediction and traffic signal control system for smart city. Soft Comput 2021. https://doi.org/10.1007/s00500-021-05896-x.
[31] Alotaibi Y, Alghamdi S, Khalaf OI, Ulaganathan S. Improved metaheuristics-based clustering with multihop routing protocol for underwater wireless sensor networks. Sensors 2022;22:1618. https://doi.org/10.3390/s22041618.
[32] Luo X, Kang L, Lu C, Linghu J, Lin H, Hu B. An enhanced multicell-to-multicell battery equalizer based on bipolar-resonant LC converter. Electronics 2021;10:293.
[33] Xu P, Li J, Sun C, Yang G, Sun F. Adaptive state-of-charge estimation for lithium-ion batteries by considering capacity degradation. Electronics 2021;10:122.
[34] Ko Y, Choi W. A new SOC estimation for LFP batteries: application in a 10 Ah cell (HW 38120 L/S) as a hysteresis case study. Electronics 2021;10:705.
[35] Samanta A, Chowdhuri S. Active cell balancing of lithium-ion battery pack using dual DC-DC converter and auxiliary lead-acid battery. J Energy Storage 2021;33:102109.
[36] Gabbar HA, Othman AM, Abdussami MR. Review of battery management systems (BMS) development and industrial standards. Technologies 2021;9:28.